ACES

DOI: 10.1002/asia.201403409

CHEMISTRY
AN ASIAN JOURNAL
Full Paper

Medicinal Chemistry

Rational Design of Selenadiazole Derivatives to Antagonize Hyperglycemia-Induced Drug Resistance in Cancer Cells

Yuedan Liu, Yi Luo, Xiaoling Li,* Wenjie Zheng, and Tianfeng Chen*[a]

Abstract: Hyperglycemia is an important factor for chemoresistance of hepatocellular carcinoma patients with diabetes to therapeutics. In the present study, a series of selenadiazole derivatives have been rationally designed, synthesized, and found be able to antagonize drug resistance in HepG2 cells to doxorubicin (DOX) under simulated diabetes conditions. Hyperglycemia could promote the cell proliferation through upregulation of ERK and AKT phosphorylation. However, the synthetic selenadiazole derivatives effectively potentiated the cellular uptake of DOX and enhanced the antiproliferative activity of DOX on HepG2 cells by induction of apoptosis, via regulation of ROS-mediated AMPK activation, inhibition of mTORC1, and an increase in DNA damage. The selenadiazole derivatives that possess an increased lipophilicity could enhance the cellular uptake and anticancer efficacy of DOX. Taken together, this study provides a rational design strategy of selenadiazole derivatives to overcome hyperglycemia-induced drug resistance.

Introduction

Hepatocellular carcinoma (HCC) is one of the most common malignant diseases worldwide; it is difficult to diagnose at an early stage and lacks cure when diagnosed at a late stage.[1] Infection with hepatitis B or C virus, alcohol and non-alcoholic fatty liver disease, and diabetes mellitus (DM) are the major risk factors of HCC.[2] The therapeutic options fall into five main categories: surgical interventions, percutaneous interventions, transarterial interventions, radiation therapy and drugs, as well as gene and immune therapies.[3] Many issues still exist after successful HCC resection, and tumor recurrence in about 62.5% of patients after 5 years is a major clinical problem.[4] Furthermore, the fact that HCC is resistant to conventional chemotherapy or radiotherapy leaves this disease with no effective therapeutic options and a very poor prognosis.[5] However, a new therapeutic platform which combines regular chemotherapy with radiation therapy can minimize side effects as well as increase drug-delivery efficiency.[6] Single-agent chemotherapy such as cisplatin, 5-fluorouracil (5-FU), and doxorubicin (DOX) have been reported to cause a response rate of 10–20%. DOX is perhaps the most widely used agent in HCC, but it has hematologic and gastrointestinal toxicities.[7]

As well as predilection sites of tumor, liver is also a vital organ for energy metabolism whose functional changes play an important role in DM. DM has become a very common health problem and is one of the most common comorbid illnesses which were found in patients with HCC.[8] According to published statistics, 47% of patients with HCC have DM.[8b] DM characteristics are hyperglycemia, hyperinsulinemia, and insulin resistance.[9] The latest statistics show that HCC with DM is increasing and that such patients are often not sensitive to chemotherapy; accordingly, their prognosis is poor.[10] Hyperglycemia is an important clinical manifestation of DM and one important reason for why HCC patients with DM are not sensitive to chemotherapy. Therefore, rational design of drugs that could reverse hyperglycemia-induced drug resistance could contribute significantly to cancer therapy.

Selenium (Se) acts as an essential element playing an important role in maintaining the health of human beings. Epidemiological, clinical studies also support the role of Se compounds as potent antitumor drugs.[11] Many studies have shown that Se-containing complexes lead to high selectivity between cancer cells and normal cells.[12] Compared with inorganic selenium, organoselenium compounds are of lower biochemical cellular toxicity. Following the development of organoselenium compounds, they have been used as antitumor agents, antioxidants, enzyme inhibitors, anti-infective agents, and cytokine inducers.[13] Organoselenium compounds are advantageous relative to inorganic selenium compounds as they can be generated under relatively mild reaction conditions and avoiding protection group chemistry.[14] Among the organoselenium compounds, selenadiazole derivatives possess the highest anticancer activity. For instance, Plano et al. synthesized fourteen substituted selenadiazole derivatives, and they all exhibited good antiproliferative and cytotoxic activities in vitro, espe-

[a] *Y. Liu,[+] Y. Luo,[+] Dr. X. Li, Dr. W. Zheng, Dr. T. Chen*
Department of Chemistry
Jinan University
Guangzhou 510631 (P. R. China)
E-mail: tlxlli@jnu.edu.cn
tchentf@jun.edu.cn

[+] *These authors contributed equally to this work.*

Supporting information for this article is available on the WWW under http://dx.doi.org/10.1002/asia.201403409.

cially against breast (MCF-7) cancer cells.[15] Chen et al. have synthesized 1,2,5-selenadiazolo-[3,4-d] pyrimidine-5,7-(4*H*,6*H*)-dione (SPO) and anthrax-[1,2-c]-[1,2,5]-selenadiazolo-6,11-dione (ASDO). SPO induced apoptosis of MCF-7 cells by activation of caspase-8 and caspase-9, overproduction of reactive oxygen species (ROS), and depletion of mitochondrial membrane potential ($\Delta\Psi$m) through regulating the expression of Bcl-2 family members, while ASDO induced caspase-dependent and ROS-independent apoptosis in MCF-7 cells in a p53-dependent manner.[11] Zhou et al. synthesized selenadiazole derivatives that act as novel radiosensitizer which can enhance X-ray treatment to induce G2/M arrest in cancer cells.[16] In our previous study we demonstrated that selenocysteine (SeC) can enhance the apoptosis induced by first-line antitumor drugs such as DOX, 5-FU, and auranofin (AF) by overproduction of ROS, activation of the Bcl-2 family, and inactivation of Akt and extracellular regulated protein kinases (ERKs).[17] These results suggested that organoselenium compounds have antagonizing drug-resistance potential on hyperglycemia. Therefore, the aim of our current study is to clarify whether hyperglycemia has an impact on the antitumor activity of DOX and to then evaluate the synergistic effects of selenadiazole derivatives and DOX on HCC cells. Furthermore, we focus on the antitumor mechanisms including the adenosine monophosphate-activated kinase (AMPK) pathway and ROS-mediated DNA damage on hyperglycemia. This study may provide an effective strategy to design selenadiazole derivatives with potency to overcome hyperglycemia-induced drug resistance (Figure 1).

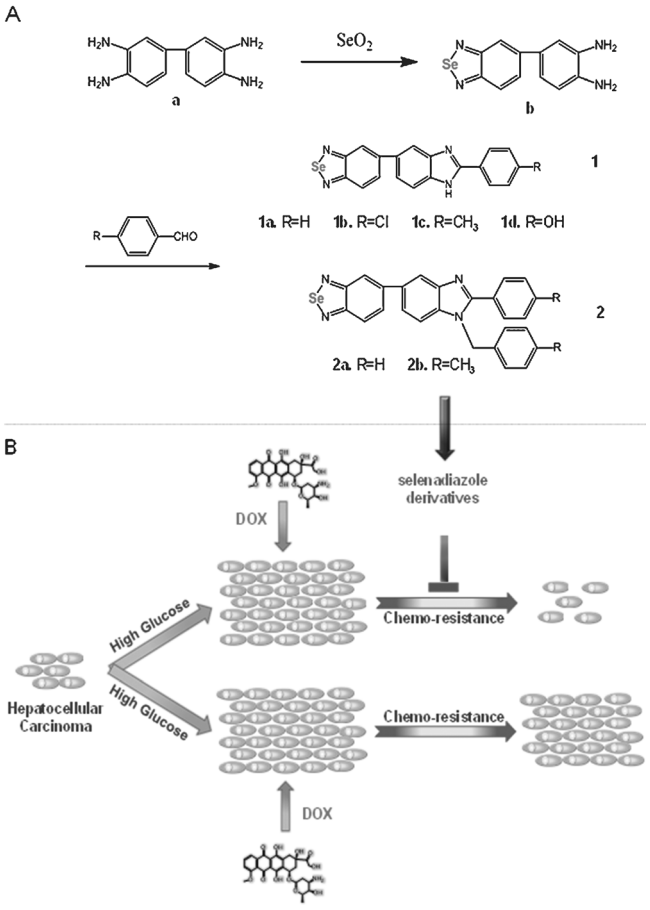

Figure 1. (A) Synthetic route for **1a**–**1d** and **2a**–**2b**. (B) Selenadiazole derivatives antagonize hyperglycemia-induced drug resistance in HepG2 hepatocellular carcinoma cells.

Results and Discussion

Hyperglycemia Induces Chemoresistance

Three major mechanisms have been proposed to explain the possible promoting impact of DM on cancer: hyperglycemia, activation of the IGF signaling pathway, and activation of the insulin signaling pathway.[18] Glucose is vital for cell survival, however, the function of glucose regarding the viability of HCC cells has not yet been defined. To this end, we maintained HepG2 cells were in Dulbecco's modified Eagle's medium (DMEM, glucose-free) with added glucose at various concentrations. The concentrations of glucose were selected according to the physiological conditions in healthy and diabetic individuals. The diagnostic fasting plasma (blood) glucose value has been lowered to $\leq$7.0 mM.[19] As a result of the normal blood glucose concentration range from 3.89 to 6.11 mM, the formation and development of a tumor is a constant process to overcome the lack of oxygen and nutrient-deficient environment. Tumor cells use the glucose and improve their glycolysis to maintain their survival and growth. Normal blood glucose levels averaging 5 mM conditions can be regarded as an energy shortage for tumor growth conditions. A higher level of 25 mM is beneficial to the growth of tumor cells, as confirmed by a large number of tumor cell culture experiments.[10] The glucose concentrations of 2.78 and 5.5 mM represent hypoglycemia and normoglycemia, while 11 mM and 25 mM of glucose are recognized as hyperglycemia. The results showed that with increasing glucose concentration, the proliferation of HepG2 cells is increasing. At a glucose concentration of 5.5 mM, HepG2 cells showed a similar rate of proliferation as in hypoglycemia (Figure 2A). To further investigate whether the proliferation is related to the proliferin in the signaling pathway, we evaluated the expressions of ERK and Akt. As shown in Figure 2B, the expressions of ERK and Akt are increased after treatment with higher glucose concentrations. These data suggested that hyperglycemia can promote the proliferation of HepG2 cells, which has a positive correlation with the expression of proliferin.

In our study, we have demonstrated that glucose can significantly promote the growth of HepG2 cells, however, it remained unclear whether hyperglycemia contributed to the chemotherapy resistance of HepG2 cells. Therefore, five anticancer drugs, that is, lomustine (CCNU), cisplatin, cyclophosphamide (CTX), DOX, and taxol were selected to test their antitumor activity. Cisplatin and DOX are known to be active cytotoxic agents in HepG2 cells, with DOX having the best anticancer activity (Table S1, Supporting Information). Upon incubation at a glucose concentration of 25 mM for 48 h, the IC_{50} is 2 μM which is higher than the value of 1.14 μM under treatment at 5.5 mM glucose (Figure 2C). Taken together, DOX has better antitumor effects among the tested antitumor agents in

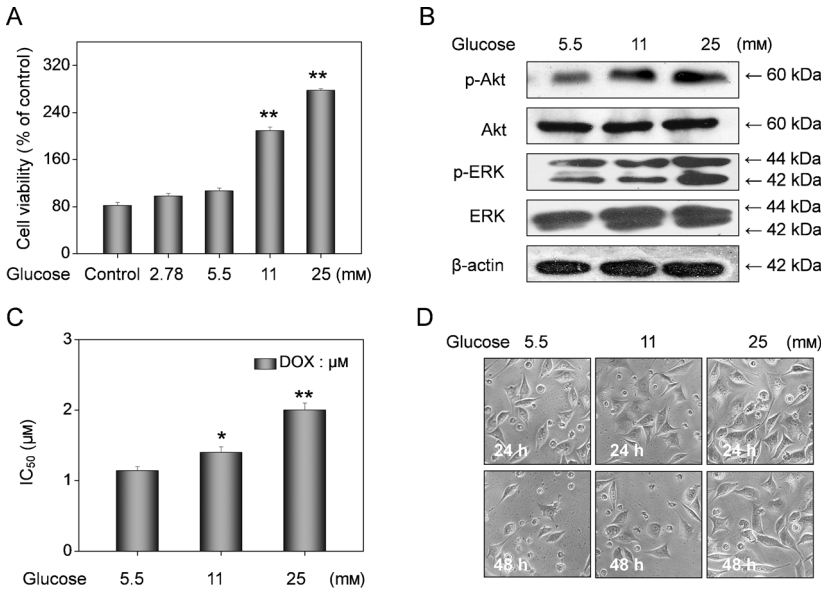

Figure 2. Glucose promotes the proliferation of hepatocellular carcinoma HepG2 cells and impairs its response to DOX. (A) Glucose promotes the proliferation of HepG2 cells. The cells were incubated for 48 h in the absence and presence of different concentrations of glucose, and the cell viability was determined by MTT assay. (B) Effects of different glucose concentrations on the phosphorylation status and the expression level of Akt and ERK. (C) The IC_{50} values of DOX in HepG2 cells were determined by using the MTT assay at different glucose concentrations following incubation for 48 h. (D) Light microscopy images of cells after treatment with DOX (1 μM) at different concentrations of glucose for 24 h and 48 h, respectively. The data shown in panels A and C represent the means ± SD of three independent experiments. *, $P < 0.05$; **, $P < 0.01$ versus the control.

HepG2 cells, but hyperglycemia-induced DOX resistance remained significant.

Rational Design and Anticancer Efficacy of Selenadiazole Derivatives

Although anticancer effects of DOX have been frequently reported, the cardiomyopathy of DOX limited its use in clinical therapy.[20] Therefore we need to find a strategy to reverse chemotherapy resistance to DOX in order to achieve better anticancer activities. Several studies have reported that organoselenium compounds can sensitize cancer cells to DOX-induced apoptosis.[21] Several reports suggested that DOX-induced apoptosis is mediated by the formation of ROS and p53 phosphorylation.[22] Selenium particles have been reported to possess low toxicity and excellent anticancer activity.[23] The selenium-induced apoptosis has been regarded as ROS-mediated mitochondria dysfunction and p53 phosphorylation.[24] Thus, we designed and synthesized a series of novel selenadiazole derivatives to overcome hyperglycemia-induced drug resistance of HepG2 HCC cells. The synthesized selenadiazole derivatives were characterized by IR spectroscopy, ESI mass spectrometry, elemental analysis, and ^{1}H NMR spectroscopy (see the Experimental Section for further details and Figures S1–S12 in the Supporting Information). The physicochemical properties (melting point and lipophilicity) of these selenadiazole derivatives were also examined.

Six novel benzo[c][1,2,5]selenadiazole derivatives were synthesized as shown in Figure 1 A. The cell viability in the presence of these compounds was tested by MTT assay, and IC_{50} values were calculated as described in the Experimental Section. As shown in Figure 3 B, **1 b** exhibited significant anticancer activity in HepG2 cells among the six benzo[c][1,2,5]selenadiazole derivatives, followed by **2 a**. However, as shown in Table S2 in the Supporting Information, relative to **1 b**, the toxicity of **2 a** toward human glandular kallikrein-2 (HK-2) cells (IC_{50} value > 400 μM) was much lower. The lipophilicity (log*P*) and cell cytotoxicity are the key factors for evaluating the efficacy of anticancer drugs.[25] Thus, the six selenadiazole derivatives were examined in both aspects. As shown in Figure 3 A, the difference in log*P* is due to their dissimilar functional groups. An insignificant connection between the activity and electronic effects could be observed as to electron-donating and -withdrawing groups. The compound **2 b** results in the highest distribution coefficient among those six selenadiazole derivatives, and the log*P* of **2 a** is second, followed by **1 b** (containing the functional group Cl). The log*P* of the other compounds was lower, revealing its lower solution in the oil phase. Meanwhile, the ratio of reactants could be an influencing

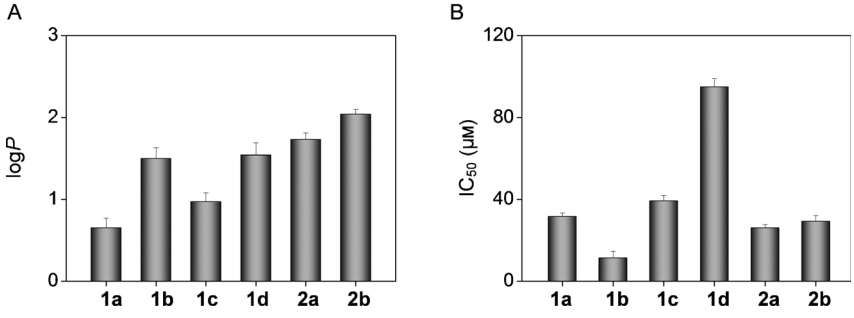

Figure 3. The lipophilicity (log*P*) of benzo[c][1,2,5]selenadiazole derivatives and their IC_{50} values. (A) The distribution of complexes in *n*-octanol and the aqueous phase using the "shake-flask" method. (B) Cells were treated with various concentrations of tested compounds for 48 h. Cell viability was determined by MTT assay, and IC_{50} values were calculated as described in the Experimental Section. Each point represents the mean ± SD of three independent experiments.

factor. The reaction products of 1 mmol **b** and 2 mmol of the corresponding aromatic aldehyde were of relatively high activity and proper lipid partition.

As shown in Figure 3A and 3B, **2a**, and **2b** have a higher solubility than other selenadiazole derivatives and possess a good anticancer effect. Compound **2a** exhibited a high lipophilicity (log*P* = 1.74), low IC_{50} value (25.68 μM) in HepG2 cells, and low toxicity toward HK-2 cells (IC_{50} > 400 μM), which indicated that **2a** has an increased potential to overcome hyperglycemia-induced drug resistance compared to the other selenadiazole derivatives. The results showed that the increase in log*P* may be concerned with a high solubility on lipids, which probably facilitates their crossing of the cell membrane and their entry into tumor cells, thus improving their anticancer efficacy. In summary, the cytotoxicities of the selenadiazole derivatives toward cancer cells were entirely different.

Cellular Uptake and Apoptosis-Inducing Efficacy

Next, we compared the antitumor activity of **2a** toward HepG2 cells at concentrations of 5 μM, 10 μM, and 20 μM in the presence of glucose at concentrations of 5.5 mM, 11 mM, and 25 mM, respectively. As shown in Figure 4A, at 5 μM **2a**, the cell viability steadily increased from 63.8% to 71.4% with increasing glucose concentration. A similar trend was found at the two higher drug concentrations. The cell viability was determined by MTT assay after treatment with **2a** and/or DOX for 48 h. As shown in Figure 4B, **2a** enhanced the cell growth inhibitory effects of DOX in HepG2 cells: compared to single treatment with a specific concentration of **2a** (control), the cell viability was decreased upon combined **2a**/DOX treatment. For instance, the cell viability of HepG2 cells treated with **2a** at 2.5 μM was 82%, while that treated with **2a** (2.5 μM) and DOX (0.625 μM) was 61%. The results showed that treatment of HepG2 cells with **2a** alone caused less inhibition of cellular proliferation than the combination of **2a** and DOX. To assess whether the mode of anticancer action in HepG2 cells of **2a** and DOX was additive or synergistic, the proliferation inhibitory effects were examined by MTT assay and then analyzed by the isobologram method.[26]

Compared with the individual treatment, the in vitro anticancer activities of **2a** and DOX at different ratios (5:4 and 5:1, w/w) were investigated. The IC_{50} values of **2a** and DOX alone in HepG2 cells are 25.68 μM and 2 μM, respectively. The combination index (CI) of **2a** and DOX was calculated as 0.4. The results of the isobologram analysis revealed that the growth inhibitory effect by **2a** and DOX was strongly synergistic, as the location of the data point in the isobologram is far below the line defining an additive effect (Figure 4C). Taken together, our results demonstrated that the combination treatment of **2a** and DOX could be a better way to enhance the anticancer efficacy in HepG2 cells. Moreover, based on the MTT assay results, the combination of **2a** and DOX (ratio = 4:1) was selected as an optimized condition for further study. Cellular uptake is an important factor contributing to anticancer activity. The increase in log*P* indicates an enhanced cellular uptake, thus improving anticancer efficacy. In this study, DOX has a strong red autofluorescence while **2a** is green fluorescent. Accordingly, the drug uptake into cells can be directly monitored. Therefore, a quantitative analysis was conducted by using a fluorescence microplate reader to measure the cellular uptake of **2a** and DOX in HepG2 cells. It was found that the intracellular drug concentration increased in a time- and dose-dependent manner in the cancer cells. As shown in Figure 4D, after 12 h incubation with **2a** followed by treatment with DOX for 4 h, the intracellular DOX concentration was 18.8 μM/10^8 cells, which was about 2–3 times higher than that following treatment with **2a** or DOX alone. Compound **2a** significantly promoted the uptake of DOX in a time-dependent manner; however, treatment with DOX alone can cause a slight increase in HepG2 cells, indicating the important role of **2a**. The intracellular trafficking of **2a** and DOX can be monitored by fluorescence imaging

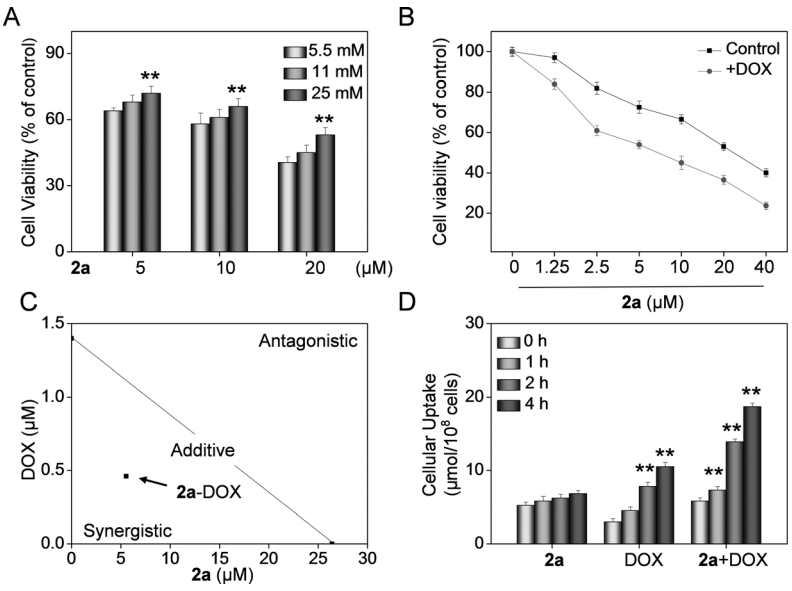

Figure 4. Compound **2a** enhanced the cellular uptake and apoptosis-inducing efficacy of DOX in HepG2 cells. (A) Cells were treated with **2a** for 48 h in DMEM containing 0 mM (control), 5.5 mM, 11 mM, and 25 mM glucose, respectively, and the cell viability was determined by MTT assay. (B) Cell viability was determined by MTT assay after treatment with 0.625 μM DOX for 48 h (squares) or pre-treatment with 2.5 μM **2a** for 12 h followed by incubation with 0.625 μM DOX for 24 h (circles) The data show that **2a** enhances the cell growth inhibitory effects of DOX on HepG2 cells. (C) Isobologram analysis of the antiproliferative effects of **2a** and/or DOX on HepG2 cells. (D) HepG2 cells were pre-treated with **2a** (20 μM) for 12 h and then treated with DOX (4 μM) at 37 °C for different times. The cellular uptake was determined as described in the Experimental Section. Each data point represents the mean ± SD of three independent experiments. *, $P < 0.05$; **, $P < 0.01$ versus the control.

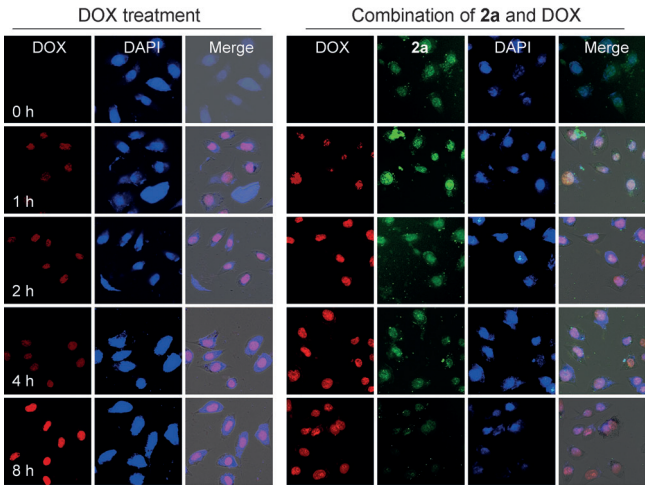

Figure 5. Compound **2a** enhanced the cellular uptake of DOX and induces apoptosis in HepG2 cells. HepG2 cells were pre-treated with **2a** (20 μM) for 12 h and then treated with DOX (4 μM) for different times. Cells were then stained with DAPI (nuclei) at 37 °C for 1 h and visualized under a fluorescent microscope.

to determine the location of compounds. DAPI (blue) is a special fluorescent tracer, which was used to label the nuclei. The change of DOX fluorescence from the cytoplasm in HepG2 cells further confirmed the sensibilization of the antitumor effect of **2a**. As shown in Figure 5, relative to a single treatment with DOX, the results of fluorescence microscopy showed that upon pre-treatment with **2a** for 12 h followed by treatment with DOX for 1–8 h, which accumulates in the cell after 1 h, the amount of internalized DOX increased in a time-dependent manner. This result indicates that pre-treatment with **2a** caused a faster aggregation of DOX in the cytoplasm.

Apoptosis Signaling Pathways Induced by 2a and DOX

In order to investigate the mechanism underlying the death of HepG2 cells induced by **2a** and/or DOX, propidium iodide (PI) staining followed by flow cytometric analysis was used to determine the apoptotic sub-G1 fraction in the treated cells. As shown in Figure 6A, PI-flow cytometric analysis of cells treated with **2a** (2.5 μM) or DOX (0.625 μM) alone increased cell apoptosis from 1.2% to 31% and 8.8%, respectively, at a glucose concentration of 5.5 mM. However, the combined treatment with **2a** (2.5 μM) and DOX (0.625 μM) caused 69.2% of cell apoptosis at the same glucose concentration. Similarly, at 25 mM glucose, single treatment with **2a** (2.5 μM) or DOX (0.625 μM) resulted in subG1 fractions of 22.3% and 5.4%, respectively, whereas the combined **2a**/DOX treatment caused 47.5% of cell apoptosis. These data clearly showed that high glucose concentrations enhance the resistance to **2a** and/or DOX in HepG2 cells (Figure 6B). Since **2a** could amplify the in vitro anticancer and apoptosis-inducing effects of DOX, we next conducted further studies to evaluate the molecular mechanism by which **2a** sensitizes the cancer cells to DOX. Caspases play a role as mediators of apoptosis by cleavage to activate various cellular substrates. In this study, a fluorometric assay was used to measure the protein activation of executor caspases, that is, caspase-3, caspase-8 (Fas/TNF-mediated), and caspase-9 (mitochondrial-mediated). As shown in Figure 6C, treatment with **2a** or DOX alone slight-

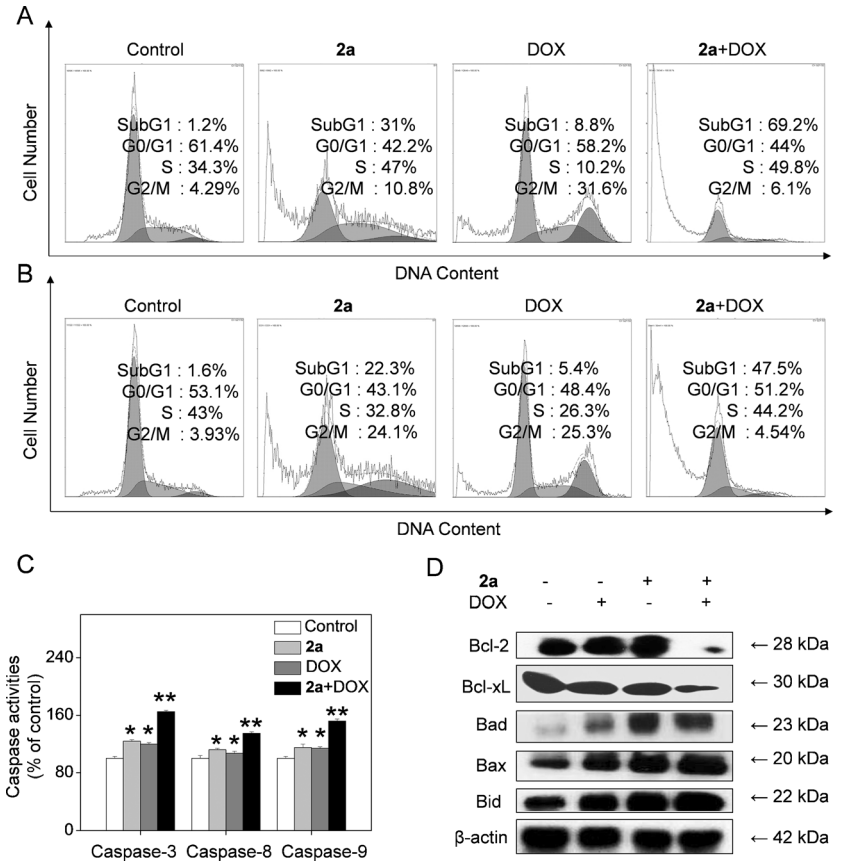

Figure 6. Compound **2a** enhanced DOX-induced apoptosis by regulating the expression of Bcl-2 family proteins. (A,B) **2a** (2.5 μM) enhanced DOX (0.625 μM)-induced apoptosis in HepG2 cells. After treatment with 5.5 mM and 25 mM glucose for 36 h, cells were harvested and fixed with 70% ethanol before being stained with PI. Apoptotic cells with hypodiploid DNA content were measured by quantifying the sub-G1 peak. (C) Analysis of caspase activity in HepG2 cells treated with **2a** and/or DOX. HepG2 cells were pre-treated with 2.5 μM **2a** for 12 h and then treated with 2.5 μM DOX for 24 h. Caspase activities were determined by using synthetic fluorogenic substrates. (D) Western blot analysis of the expression levels of Bcl-2, Bcl-xL, Bad, Bax, and Bid in HepG2 cells. Equal protein loading was confirmed by analysis of β-actin in the protein extracts. Similar results were obtained from three independent experiments.

ly increased the activation of caspase-3/8/9, indicating that either **2a** or DOX can also induce extrinsic death receptor-mediated apoptotic pathways. By contrast, the combined treatment of **2a** and DOX synergistically enhanced the activation of caspase-3/8/9. Taken together, these results demonstrate the contribution of extrinsic and intrinsic pathways to cell apoptosis.

Mitochondria integrity is central to both extrinsic and intrinsic apoptosis signals induced by the accumulation of ROS and consequently changed the cellular redox state.[17a,27] Depletion of the mitochondrial membrane potential ($\Delta\Psi$m) and release of apoptogenic factors from the mitochondria into the cytoplasm will cause apoptosis and is lethal to the cells. Bcl-2 family proteins, the key regulators of $\Delta\Psi$m, also have been described as critical regulators of the mitochondrial apoptosis pathway. The mitochondrial apoptosis pathway ensures that cell death is controlled by the leakage of pro-apoptotic proteins from the intermembrane space of mitochondria under the tight regulation of the Bcl-2 family that comprise both anti-apoptosis factors, such as Bcl-2 and Bcl-xL, and pro-apoptosis proteins, such as Bax, Bad, and Bid.[28] Once the balance is disrupted, apoptosis will be initiated via the mitochondrial-mediated pathway. The Bcl-2 and Bcl-xL proteins are overexpressed in many cancer cell types and contribute to the chemotherapy and radiation therapy resistance in cancer cells.[29] Therefore, an obvious decrease in the Bcl-2/Bax and Bcl-xL/Bad expression could be a primary mechanism by the combined treatment of **2a** and DOX inducing mitochondria-mediated apoptosis in HepG2 cells. Western blotting was applied to examine the expressions of pro-survival and pro-apoptotic Bcl-2 family proteins in HepG2 cells, which can provide evidence of the effects of **2a** and DOX. As shown in Figure 6D, the treatment with **2a** and DOX decreased the expression level of the anti-apoptotic proteins Bcl-xL and Bcl-2, whereas it increased the expression levels of the pro-apoptotic proteins Bad and Bax. Truncation of Bid (tBid) leads to an activated form of Bid which has potent pro-apoptotic activity. The activation of Bid could translocate Bax from the cytoplasm to the mitochondrial membrane and then induce aggregation.[28] The combined treatment of HepG2 cells with **2a** and DOX caused a significant increase in tBid that confirmed the activation of the extrinsic apoptosis pathway. Taken together, these results demonstrated that the sensitization of DOX-induced apoptosis by **2a** is correlated with the expression levels of Bcl-2/Bax, Bcl-xL/Bad, and tBid. These results suggest that mitochondria could be the intracellular targeting organelle of selenadiazole derivatives. Mitochondria are pivotal in controlling cell growth and death. We observed the changes of mitochondria (stained by Mito-Tracker; nuclei stained by DAPI) in HepG2 cells treated with **2a** and/or DOX. As shown in Figure 7, obvious mitochondrial fragmentation could be observed after treatment for 2 h.

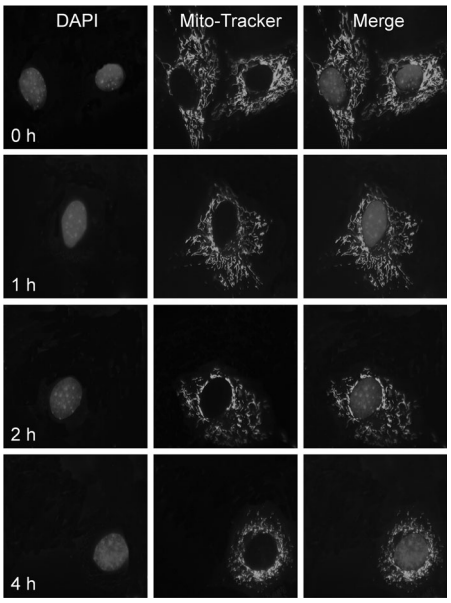

Figure 7. Treatment with **2a** and DOX caused mitochondrial fragmentation in HepG2 cells. Representative photomicrographs of mitochondria fragmentation and nuclear condensation induced by **2a** (2.5 μM) and DOX (0.625 μM) at different periods of time using a MitoTracker–DAPI co-staining assay.

ROS Overproduction

ROS are well known to be produced from the normal cellular oxygen metabolism and mainly include hydrogen superoxide, peroxide, and hydroxyl radicals; they are involved in cancer cell apoptosis induced by chemotherapeutic agents and radiotherapy.[30] DOX-induced cell apoptosis or cell cycle arrest is mostly viewed as the generation of ROS nowadays.[31] The overproduction of ROS induced by DOX in many cancer cells including HepG2 cells has been previously reported by our group.[32] Therefore, we examined whether **2a** has the ability to trigger ROS generation that would enhance the apoptosis signal induced by DOX by measuring the fluorescence intensity of 2′,7′-dichlorofluorescein (DCF). The results showed that pre-treatment of HepG2 cells with **2a** led to a rapid increase in ROS generation which is much higher than that upon treatment with **2a** or DOX alone (Figure 8A). To further confirm the important role of ROS generation in cell apoptosis, we next investigated the intracellular fluorescence intensity of DCF in HepG2 cells treated with **2a** and/or DOX. As shown in Figure 8B, pre-treatment of **2a** followed by incubation with DOX significantly enhanced the fluorescence intensity. Taken together, these results suggested that **2a** synergized with DOX to induce apoptosis of HepG2 cells in a ROS-dependent manner. Generally, overproduction of ROS could act on protein modification and DNA damage-activated p53 signaling pathways, which could trigger cell apoptosis.

AMPK Signaling Pathway

The mechanisms of DM that promote the development of HCC are unknown. However, many researchers have inferred that oxidative stress is the key event in the pathogenesis and complications of DM as a result of hyperglycemia.[33] Glucose uptake occurs primarily by phosphoinositide kinase-3 (PI3K) activation and enhancement of GLUT-1 expression.[34] Processes in normal cells and the proliferation of tumor cells both need

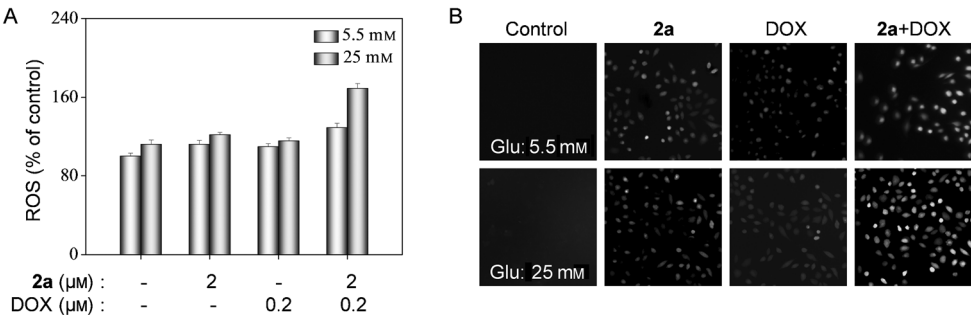

Figure 8. The role of intracellular ROS generation in apoptosis of HepG2 cells induced by **2a** and/or DOX. (A) Cells were exposed to **2a** (2 μM) and/or DOX (0.2 μM), and the level of the intracellular ROS was analyzed by measuring the fluorescence intensity of DCF. (B) Changes in the fluorescence intensity induced by **2a** (2 μM) and/or DOX (0.2 μM) in HepG2 cells. The fluorescence intensity was detected by fluorescence microscopy of DCF. Glu, Glucose.

energy. Furthermore, the tumor cell generation must evade the checkpoint under the abnormal tumor microenvironment. The main mechanism is regarded as Warburg effect in tumor cells, which is a shift from ATP generation through oxidative phosphorylation to ATP generation through glycolysis, even under the conditions of normal oxygen concentrations. This effect is regulated by p53, PI3K, and AMPK-liver kinase B1 (LKB1) pathways as well as hypoxia-inducible factor (HIF) and MYC.[35] AMPK is a serine/threonine protein kinase, which serves as a regulator of energy metabolism in all eukaryotic cell types. Several studies indicated that the activation of AMPK strongly suppresses cell proliferation in normal cells and in tumor cells.[36] Activation of AMPK requires LKB1, which is well recognized as a tumor suppressor. Many reports proposed that AMPK is an emerging drug target, probably because of mitochondrial dysfunction in type-2 diabetes, suggesting that AMPK-mediated mitochondrial improvement may overcome the metabolic sensitivity and insulin resistance.[37] To investigate whether DOX-induced apoptosis enhanced by **2a** affected the mammalian target of the rapamycin (mTOR) signaling pathway, we detected the signaling by assessing the expression of mTOR kinase, p70S6 kinase (p70S6K), eIF4E-binding protein1 (4E-BP1), and other related proteins. As shown in Figure 9B, the phosphorylation of AMPKα (Thr172) was significantly increased in HepG2 cells treated with **2a** alone, and the combination of **2a** and DOX caused even higher activation. However,

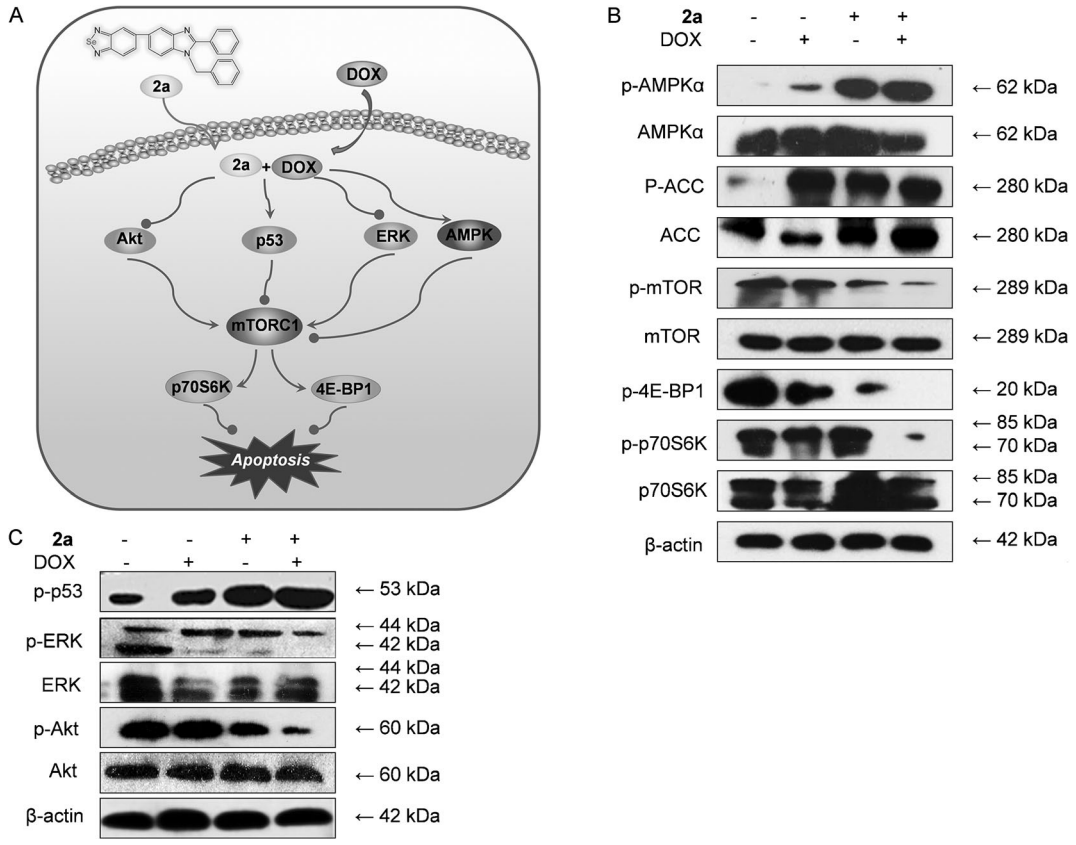

Figure 9. Mechanisms underlying the induction of apoptosis upon treatment of HepG2 cells with **2a** and/or DOX. (A) Schematic illustration of DOX (0.625 μM)-induced apoptosis of HepG2 cells enhanced by **2a** (2.5 μM. (B, C) **2a** (2.5 μM) and DOX (0.625 μM) induced apoptosis via the AMPK signaling pathway and its upstream kinase in HepG2 cells. Equal protein loading was confirmed by analysis of β-actin in the protein extracts.

treatment by DOX alone only slightly activated the expression of AMPKα. The activation of AMPKα can inhibit the expression of mTOR (Ser2448) by TSC (tuberous sclerosis complex) and downregulate the expression of p70S6K (Ser371) and 4E-BP1 (Thr37/46), leading to cell growth inhibition and apoptosis. The expression levels of mTOR and 4E-BP1 were decreased slightly after treatment with DOX alone, while they were significantly downregulated by **2a** and co-treatment, which indicated an important role of **2a** in the induction of apoptosis. These results indicated that **2a** promoted largely the DOX-induced apoptosis in HepG2 cells via the AMPK signaling pathway. Several lines of evidence suggest that organoselenium compounds cause cell death via activating the p53 signaling pathway and induced ROS-mediated DNA damage.[38] DOX-induced apoptosis is known to be dependent on p53.[21] The tumor suppressor protein p53 is a transcription factor that plays a critical role in cell-cycle arrest and apoptosis by regulating the expression of a variety of genes located upstream in the mTOR signaling pathway. Phosphorylation of p53 at Ser15 can induce cells apoptosis upon treatement with many anticancer drugs. To investigate whether cell apoptosis induced by **2a** and/or DOX was regulated by the p53 pathway, we examined the phosphorylation status of p53 in HepG2cells. As shown in Figure 9C, treatment of HepG2 cells with DOX resulted in insignificant p53 activation. By contrast, the treatment with **2a** alone or in combination with DOX significantly upregulated the expression level of phosphorylated p53. Akt and ERK, the up-stream kinases of mTORC1, were also activated after treatment with **2a** and/or DOX. Taken together, **2a** enhanced DOX-induced apoptosis mainly by activation of the AMPK-mTORC1-p70S6K and AMPK-p53 signaling pathways. Here, we propose a general apoptosis pathway for the action of these two drugs on signal mediators in HepG2 cells (Figure 9A). From the analysis above we can propose a signaling network for the synergistic action of **2a** and DOX. Pre-treatment with **2a** enhanced the cellular uptake of DOX, which subsequently increased the generation of intracellular ROS and DNA damage and triggered the p53 pathway, causing mitochondrial dysfunction by regulating the expressions of Bcl-2 family proteins, which finally activated the AMPK signaling pathway. p53 is an upstream factor of the AMPK signaling pathway. Mitochondrial dysfunction results in the leakage of apoptogenic factors into the cytosol, which subsequently activated several caspase cascades, finally inducing cell apoptosis. In addition, ROS led to inactivation of Akt, promoted the phosphorylation of AMPK, and changed the status of its downstream kinase. The present study demonstrated that **2a** results in ROS generation and, interestingly, pretreatment of HepG2 cells with **2a** significantly enhanced DOX-induced apoptosis through triggering ROS overproduction. Relative to DOX, **2a** performed better in the activation of the AMPK signaling pathway to induce cell apoptosis, though the combination treatment of **2a** and DOX caused a greater response in HepG2 cells. Therefore, phosphorylation of Akt and AMPK, and the inactivation of mTOR may be incurred by ROS and potentiated the apoptosis cascade in this synergism (Figure 10).

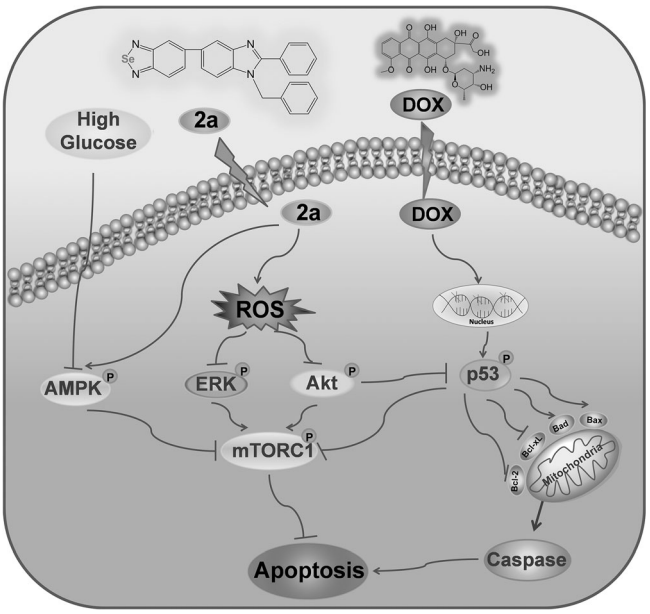

Figure 10. Proposed apoptotic signaling pathways of DOX-induced apoptosis of HepG2 cells enhanced by **2a**. DOX causes DNA damage by activation of p53, whereas **2a** synergistically activated AMPK and then inactivates mTORC1 by inducing intracellular ROS generation and inactivation of Akt and ERK. Thus, the DOX-induced DNA damage is enhanced, resulting in further activation of the p53 pathway, which in turn triggeres mitochondrial dysfunction to amplify the apoptotic signals.

Conclusions

In this study, we demonstrate the effects of diabetes mellitus on the chemotherapy of hepatocellular carcinoma and report on new apoptosis-inducing agents with low toxicity. Firstly, we show that hyperglycemia promotes the proliferation of HepG2 cells. Secondly, we reveal that hyperglycemia inhibits the chemotherapeutic effects of antitumor drugs such as DOX. By contrast, selenadiazole derivatives, in particular **2a**, can reverse the chemotherapeutic resistance of DOX. Lastly, we elucidate the synergistic mechanisms of selenadiazole derivatives and DOX to induce apoptosis in HepG2 cells. Taken together, we have rationally designed a series of selenadiazole derivatives with the potential to overcome hyperglycemia-induced drug resistance in HepG2 cells by enhancement of cellular uptake of DOX, activation of ROS-mediated DNA damage, mitochondrial fragmentation, and activation of the AMPK signaling pathway.

Experimental Section

Materials

Glucose-free Dulbecco's modified Eagle's medium (DMEM) was purchased from Gibco. D-Glucose, propidium iodide (PI), 2′,7′-dichlorofluorescein diacetate (DCF-DA), thiazolyl blue tetrazolium bromide (MTT), bicinchoninic acid (BCA) kit, doxorubicin (DOX) and 4′,6-diamidino-2-phenyindole (DAPI) were purchased from Sigma. Fetal bovine serum (FBS) and the antibiotic mixture (penicillin/streptomycin) were purchased from Invitrogen (Carlsbad, CA, USA). The caspase-3 substrate (Ac-DEVD-AMC), caspase-9 substrate (Ac-LEHD-AFC) and caspase-8 substrate (IETD-AFC) were purchased

from Calbiochem. All of the antibodies used in this study were purchased from Cell Signaling Technology (Beverly, MA, USA). All of the solvents used were of high-performance liquid chromatography (HPLC) grade. The water used for all experiments was supplied by a Milli-Q water purification system from Millipore.

Synthesis of Selenadiazole Derivatives

Synthesis of compound **b:** (1,1′-Biphenyl)-3,3′,4,4′-tetraamine (**a,** 3 mmol, 642.8 mg) was dissolved in 250 mL hydrochloric acid solution (conc. HCl/H_2O = 1:5) in a 500 mL flask. Then SeO_2 (3 mmol, 332.9 mg) dissolved in 20 mL hot distilled water was added dropwise, and the mixture was stirred for 2 h at room temperature. Subsequently, sodium hydroxide solution was used to adjust the pH to about 7.0. The mixture was then filtered to afford 4-(benzo[c][1,2,5]selenadiazol-5-yl)benzene-1,2-diamine (**b,** 2.7 mmol, 780.8 mg) in a yield of 90%.

Synthesis of **1a**–**1d**: Compound **b** (1 mmol, 289.2 mg) was dissolved in 25 mL DMF in a 50 mL flask. Then, the corresponding aromatic aldehyde (1 mmol) was added together with a catalytic amount of *p*-methylbenzene sulfonic acid. The mixture was stirred for 40 min at 80 °C. Subsequently, the mixture was poured into 200 mL saturated aqueous Na_2CO_3 and stirred for 30 min at room temperature. The mixture was then filtered to give crude product, which was purified by column chromatography on silica gel (petroleum ether/EtOAc = 5:1) to afford pure product **1a**–**1d**.

Synthesis of **2a**–**2b**: Compound **b** (1 mmol, 289.2 mg) was dissolved in 25 mL DMF in a 50 mL flask. Then, the corresponding aromatic aldehyde (R = H, 2 mmol, 212 mg; R = CH_3, 2 mmol, 240 mg) was added together with a catalytic amount of *p*-methylbenzene sulfonic acid. The mixture was then stirred for 2 h at 80 °C. Subsequently, the mixture was poured into saturated aqueous 200 mL Na_2CO_3 and stirred for 30 min at room temperature. The mixture was then filtered to give crude product, which was purified by column chromatography on silica gel (petroleum ether/EtOAc = 7:1) to afford pure product **2a**–**2b**.

Characterization of 1a–1d, 2a–2b

1a: Yield: 40%; ESI-MS: *m/z* 377.2 $[M+H^+]^+$. M.p. 328–329 °C. Elemental analysis calcd (%) for $C_{19}H_{12}N_4Se$: C, 60.81; H, 3.22; N, 14.93; found (%) : C, 60.71; H, 3.12; N, 14.99; IR (KBr): $\tilde{\nu}$ = 704,584 (Se-*N*-Se), 1159, 1074 (C–N), 1608, 1450, 1388 cm^{-1} (C=C arom); ^1H NMR (500 MHz, $CDCl_3$): δ = 7.74 (m, 3H),7.94 (m, 1H), 8.00 (m, 3H), 8.18 (m, 1H), 8.24 ppm (m, 3H).

1b: Yield: 45%; ESI-MS: *m/z* 409.4 $[M-H^+]^-$. M.p. 315–316 °C. Elemental analysis calcd (%) for $C_{19}H_{11}ClN_4Se$: C, 55.70; H, 2.71; N, 13.67; found (%): C, 57.05; H, 2.75; N, 13.51; IR (KBr): $\tilde{\nu}$ = 730, 584 (Se-*N*-Se), 1207, 1058 (C–N), 1635, 1486,1432 cm^{-1} (C=C arom); ^1H NMR (500 MHz, $CDCl_3$): δ = 8.04 (m, 1H), 8.17 (s, 1H), 8.21 (d, 1H), 8.24 (m, 1H), 8.27 (m, 1H), 7.06 (d, 2H), 7.38 (m, 1H), 7.68 ppm (m, 5H).

1c: Yield: 50%; ESI-MS: *m/z* 391.1 $[M+H^+]^+$. M.p. 303–304 °C. Elemental analysis calcd (%) for $C_{20}H_{14}N_4Se$: C, 61.70; H, 3.62; N, 14.39; found (%): C, 61.72; H, 3.65; N, 14.51; IR (KBr): $\tilde{\nu}$ = 729 (Se-*N*-Se), 1360 (C–N), 1610, 1560, 793 cm^{-1} (C=C arom); ^1H NMR (500 MHz, $CDCl_3$): δ = 8.12 (d, 4H), 8.03 (d, 1H), 7.94 (d, 1H), 7.71 (t, 2H), 7.39 (d, 2H), 2.40 ppm (s, 3H).

1d: Yield: 40%; ESI-MS: *m/z* 393.3 $[M+H^+]^+$. M.p. 309–310 °C. Elemental analysis calcd (%) for $C_{19}H_{12}N_4OSe$: C, 58.32; H, 3.09; N, 14.32; found (%): C, 58.20; H, 3.03; N, 14.31; IR (KBr): $\tilde{\nu}$ = 750 (Se-*N*-Se), 3480 (C–N), 1590, 1480, 804 cm^{-1} (C=C arom); ^1H NMR (500 MHz, $CDCl_3$): δ = 8.30–7.98 (m, 3H), 7.93 (d, 1H), 7.80–7.54 (m, 1H), 6.94 ppm (d, 1H).

2a: Yield: 31%; ESI-MS: *m/z* 467.3 $[M+H^+]^+$. M.p. 295–296 °C. Elemental analysis calcd (%) for $C_{26}H_{18}N_4Se$: C, 67.10; H, 3.90; N, 12.04; found (%): C, 67.05; H, 3.95; N, 12.11; IR (KBr): $\tilde{\nu}$ = 696,586 (Se-*N*-Se), 2919 (C–H), 1245, 1106 (C–N), 1633, 1469, 1400 cm^{-1} (C=C arom); ^1H NMR (500 MHz, $CDCl_3$): δ = 7.76(m, 3H), 7.93(d, 1H), 8.02(d, 1H), 8.12(s, 1H), 8.21 (s, 1H), 5.64 ppm (s, 2H).

2b: Yield: 25%; ESI-MS: *m/z* 495.3 $[M+H^+]^+$. M.p. 277–278 °C. Elemental analysis calcd (%) for $C_{28}H_{22}N_4Se$: C, 68.15; H, 4.49; N, 11.35; found (%): C, 68.2; H, 4.45; N, 11.31; IR (KBr): $\tilde{\nu}$ = 577,485 (Se-*N*-Se), 2953 (C–H), 1286, 1124 (C–N), 1630, 1550, 802 cm^{-1} (C=C arom); ^1H NMR (500 MHz, $CDCl_3$): δ = 8.19 (s, 1H), 8.13 (s,1H), 8.09–7.97 (m, 2H), 7.97–7.88 (m, 1H), 7.87–7.72 (m, 2H), 7.11 (t, 2H), 6.94 (d, 2H), 5.63 (d, 2H), 2.39 (s, 3H), 2.22 ppm (d, 3H).

Cell Lines and Cell Culture Conditions

The cell lines used in this study, HepG2 (hepatocellular carcinoma cells) and HK-2 (human glandular kallikrein-2 cells) were obtained from the American Type Culture Collection (ATCC, Manassas, VA, USA). These cell lines were cultured in DMEM medium supplemented with 10% fetal bovine serum (FBS), penicillin (100 units mL^{-1}) and streptomycin (50 units mL^{-1}) in a 37 °C humidified atmosphere containing 95% air and 5% CO_2 as described previously.[18]

MTT Assay

Cell viability was determined by MTT assay according to the published procedure.[10,39] Cells (4000 per well) were maintained in DMEM with 10% FBS. After 24 h incubation, various concentrations of glucose were added to DMEM without glucose with 0.5% FBS in parallel to replace the original DMEM after washing with phosphate buffered saline (PBS). After 48 h, the cytotoxic effect of antitumor drugs and selenadiazole derivatives was evaluated using the previously reported methods.[40]

Measurement of Lipophilicity

The partition coefficient of each selenadiazole derivative (**1a–1d, 2a–2b**), defined as log*P* = lg([solute]octanol/[solute]water), was experimentally determined by using the "shake-flask" method as previous described.[41]

Synergy Analysis

In this study, the isobologram method was used to analyze the synergistic effect between **2a** and DOX as previously described.[32,41] The extent of addition, synergism or antagonism was evaluated by combination index (CI). A CI value <1 indicates a synergistic effect between two drugs, while a CI value of 1 indicates an additive effect, and a CI value >1 indicates an antagonistic effect.

Cellular Uptake of 2a and/or DOX

A fluorescence microplate reader (Spectra Max M5, Bio-Tek) was used to quantify the cellular uptake of compounds by fluorescence intensity as described previously.[42] Cells (8000 per well; 0.1 mL) were pre-treated with **2a** for 12 h and then incubated with DOX for various periods of time at 37 °C in a CO_2 incubator. Then the protocol of the MTT assay was followed. The excitation and emission wavelengths of intracellular DOX are 430 and 485 nm, respec-

tively. Values were expressed as the percentage of the fluorescence.

Intracellular Localization of 2a and/or DOX

HepG2 cells were incubated in high glucose DMEM with 10% FBS in 2 cm cell culture dishes for 24 hat 37 °C. After 24 h, cells were pre-treated with 20 μM **2a** for 12 h at 37 °C. Then, 4 μM DOX was added to some samples, followed by incubation for the indicated times at 37 °C. After that, 1 mg mL^{-1} of DAPI was added to the dishes for 30 min. A fluorescence microscope (Nikon Eclipse 230 80i) was used to evaluate the stained cells after rinsing the cells with PBS for three times.

Determination of Cell Apoptosis

The effects of **2a** and/or DOX on the cell cycle progression and the apoptosis rate were quantified by flow cytometric analysis (Epics-XL, Beckman Coulter) following the previously described method.[43] The caspase activity was detected by fluorescence assay with specific substrates.[17c]

Mitochondria Fragmentation

Mito-Tracker Green, a fluorescent dye which can stain mitochondria in living cells, was used. First, HepG2 cells were incubated in high glucose DMEM with 0.5% FBS in 2 cm dishes with 2.5 μM **2a** and 0.625 μM DOX at 37 °C for 1 h, 2 h, and 4 h, respectively. Control experiments were conducted without **2a** and DOX. The cells were stained with Mito-Tracker (final concentration of 100 nM) for 2 h. A fluorescence microscope (Nikon Eclipse 230 80i) was used to detect mitochondria fragmentation and nuclear condensation induced by **2a** and DOX at different times.

Intracellular ROS Generation

DCF fluorescence assay was used to evaluate the effects of **2a** and/or DOX on intracellular ROS generation as previously described.[40] Briefly, HepG2 cells (10 000 cells/well) were pre-incubated in high glucose DMEM with 10% FBS for 24 h at 37 °C in a 96-well plate. Subsequently, the medium was replaced with DMEM (glucose-free) containing glucose at various concentrations, followed by incubation for another 24 h at 37 °C. Next, cells were treated with 2 μM **2a** and/or 0.2 μM DOX. After 12 h, the solution was loaded in 10 μM DCF at 37 °C for 30 min. A Tecan Safire fluorescence reader was then used to evaluate the ROS level immediately, with excitation and emission wavelengths of 488 nm and 525 nm, respectively.

Western Blot Analysis

The BCA kit was used to quantitatively detect the cellular proteins exposed to **2a** and/or DOX in HepG2 cells. Then the expression levels of proteins in HepG2 cells after treatment with **2a** and/or DOX were investigated by Western blotting as previously described.[17b]

Acknowledgements

This work was supported by National High Technology Research and Development Program of China (SS2014AA020538), Science Foundation for Distinguished Young Scholars of Guangdong Province, Natural Science Foundation of China and Guangdong Province, Research Fund for the Doctoral Program of Higher Education of China, Foundation for High-level Talents in Higher Education of Guangdong, YangFan Innovative & Entrepreneurial Research Team Project (201312H05) China Postdoctoral Science Foundation.

Keywords: apoptosis · cancer · chemoresistance · hyperglycemia · medicinal chemistry · organoselenium

[1] J. Bruix, M. Sherman, *Hepatology* **2011**, *53*, 1020 – 1022.
[2] M. M. Hassan, L. Y. Hwang, C. J. Hatten, M. Swaim, D. Li, J. L. Abbruzzese, P. Beasley, Y. Z. Patt, *Hepatology* **2002**, *36*, 1206 – 1213.
[3] a) A. Arzumanyan, H. M. Reis, M. A. Feitelson, *Nat. Rev. Cancer* **2013**, *13*, 123 – 135; b) S. Singh, P. P. Singh, L. R. Roberts, W. Sanchez, *Nat. Rev. Gastroenterol. Hepatol.* **2014**, *11*, 45 – 54.
[4] S. Y. Lee, I. T. Konstantinidis, A. A. Eaton, M. Gönen, T. P. Kingham, M. I. D'Angelica, P. J. Allen, Y. Fong, R. P. DeMatteo, W. R. Jarnagin, *HPB* **2014**, *16*, 943 – 953.
[5] L. N. Abdullah, E. K.-H. Chow, *Clin. Transl. Med.* **2013**, *2*, 3.
[6] W. Cao, Y. Gu, M. Meineck, H. Xu, *Chem. Asian J.* **2014**, *9*, 48 – 57.
[7] Q. Wang, Y.-J. Zhong, J.-P. Yuan, L.-H. Shao, J. Zhang, L. Tang, S.-P. Liu, Y.-P. Hong, R. A. Firestone, Y. Li, *J. Transl. Med.* **2013**, *11*, 192.
[8] a) H. B. El-serag, T. Tran, J. E. Everhart, *Gastroenterology* **2004**, *126*, 460 – 468; b) J. Davila, R. Morgan, Y. Shaib, K. McGlynn, H. El-Serag, *Gut* **2005**, *54*, 533 – 539; c) C. Wang, X. Wang, G. Gong, Q. Ben, W. Qiu, Y. Chen, G. Li, L. Wang, *Int. J. Cancer* **2012**, *130*, 1639 – 1648; d) W. Koh, R. Wang, A. Jin, M. Yu, J. Yuan, *British journal of cancer* **2013**, *108*, 1182 – 1188.
[9] R. D. Ferguson, R. Novosyadlyy, Y. Fierz, N. Alikhani, H. Sun, S. Yakar, D. LeRoith, *Breast Cancer Res.* **2012**, *14*, R8.
[10] Y.-H. Feng, C.-Y. Lin, W.-T. Huang, C.-L. Wu, J.-L. Fang, C.-J. Tsao, *Med. Oncol.* **2011**, *28*, 1080 – 1088.
[11] a) T. Chen, W. Zheng, Y.-S. Wong, F. Yang, *Biomed. Pharmacother.* **2008**, *62*, 77 – 84; b) T. Chen, Y.-S. Wong, W. Zheng, J. Liu, *Chem.-Biol. Interact.* **2009**, *180*, 54 – 60.
[12] a) L. Zeng, Y. Li, T. Li, W. Cao, Y. Yi, W. Geng, Z. Sun, H. Xu, *Chem. Asian J.* **2014**, *9*, 2295 – 2302; b) T. Li, Y. Yi, H. Xu, *Acta Chim. Sin.* **2014**, *72*, 1079 – 1084.
[13] G. Mugesh, W.-W. du Mont, H. Sies, *Chem. Rev.* **2001**, *101*, 2125 – 2180.
[14] a) C. W. Nogueira, G. Zeni, J. B. Rocha, *Chem. Rev.* **2004**, *104*, 6255 – 6286; b) P. Ghosh, S. S. Roy, P. Chakraborty, S. Ghosh, S. Bhattacharya, *BioMetals* **2013**, *26*, 61 – 73.
[15] a) D. Plano, E. Moreno, M. Font, I. Encio, J. A. Palop, C. Sanmartin, *Arch. Pharm.* **2010**, *343*, 680 – 691; b) Q. Guan, F. Yang, D. Guo, J. Xu, M. Jiang, C. Liu, K. Bao, Y. Wu, W. Zhang, *Eur. J. Med. Chem.* **2014**, *87*, 1 – 9.
[16] Q. Xie, Y. Zhou, G. Lan, L. Yang, W. Zheng, Y. Liang, T. Chen, *Biochem. Biophys. Res. Commun.* **2014**, *449*, 88 – 93.
[17] a) C. Fan, J. Chen, Y. Wang, Y.-S. Wong, Y. Zhang, W. Zheng, W. Cao, T. Chen, *Free Radical Biol. Med.* **2013**, *65*, 305 – 316; b) C. Liu, Z. Liu, M. Li, X. Li, Y.-S. Wong, S.-M. Ngai, W. Zheng, Y. Zhang, T. Chen, *PLoS One* **2013**, *8*, e53945; c) C. Fan, W. Zheng, X. Fu, X. Li, Y. Wong, T. Chen, *Oncotarget* **2014**, *5*, 2853 – 2863.
[18] Y. Li, X. Li, Y.-S. Wong, T. Chen, H. Zhang, C. Liu, W. Zheng, *Biomaterials* **2011**, *32*, 9068 – 9076.
[19] K. G. M. M. Alberti, P. f. Zimmet, *Diabetic Med.* **1998**, *15*, 539 – 553.
[20] A. U. Buzdar, C. Marcus, G. R. Blumenschein, T. L. Smith, *Cancer* **1985**, *55*, 2761 – 2765.
[21] S. Li, Y. Zhou, R. Wang, H. Zhang, Y. Dong, C. Ip, *Mol. Cancer Ther.* **2007**, *6*, 1031 – 1038.
[22] J. Berthiaume, K. Wallace, *Cell Biol. Toxicol.* **2007**, *23*, 15 – 25.
[23] T. Chen, Y.-S. Wong, W. Zheng, Y. Bai, L. Huang, *Colloids Surf. B* **2008**, *67*, 26 – 31.
[24] a) Y.-j. Zhou, S.-p. Zhang, C.-w. Liu, Y.-q. Cai, *Toxicol. in Vitro* **2009**, *23*, 288 – 294; b) L. He, T. Chen, Y. You, H. Hu, W. Zheng, W. L. Kwong, T. Zou, C. M. Che, *Angew. Chem. Int. Ed.* **2014**, *53*, 12532 – 12536.
[25] T. Zou, C. T. Lum, S. S. Y. Chui, C. M. Che, *Angew. Chem. Int. Ed.* **2013**, *52*, 2930 – 2933; *Angew. Chem.* **2013**, *125*, 3002 – 3005.
[26] R. J. Tallarida, *J. Pharmacol. Exp. Ther.* **2001**, *298*, 865 – 872.
[27] T.-S. Kim, B. Y. Yun, I. Y. Kim, *Biochem. Pharmacol.* **2003**, *66*, 2301 – 2311.

[28] M. Donovan, T. G. Cotter, *Biochim. Biophys. Acta Mol. Cell Res.* **2004**, *1644*, 133 – 147.
[29] H. Hikita, T. Takehara, S. Shimizu, T. Kodama, W. Li, T. Miyagi, A. Hosui, H. Ishida, K. Ohkawa, T. Kanto, *Hepatology* **2009**, *50*, 1217 – 1226.
[30] H. Pelicano, D. Carney, P. Huang, *Drug Resist. Updates* **2004**, *7*, 97 – 110.
[31] a) S. Wang, E. A. Konorev, S. Kotamraju, J. Joseph, S. Kalivendi, B. Kalyanaraman, *J. Biol. Chem.* **2004**, *279*, 25535 – 25543; b) W. Tsang, S. P. Chau, S. Kong, K. Fung, T. Kwok, *Life Sci.* **2003**, *73*, 2047 – 2058; c) C. Ji, B. Yang, Y. Yang, S. He, D. Miao, L. He, Z. Bi, *Oncogene* **2010**, *29*, 6557 – 6568.
[32] Y. Huang, L. He, W. Liu, C. Fan, W. Zheng, Y.-S. Wong, T. Chen, *Biomaterials* **2013**, *34*, 7106 – 7116.
[33] P. Rösen, P. Nawroth, G. King, W. Möller, H. J. Tritschler, L. Packer, *Diabetes/Metab. Res. Rev.* **2001**, *17*, 189 – 212.
[34] X.-Z. Ding, D. M. Fehsenfeld, L. O. Murphy, J. Permert, T. E. Adrian, *Pancreas* **2000**, *21*, 310 – 320.
[35] R. A. Cairns, I. S. Harris, T. W. Mak, *Nat. Rev. Cancer* **2011**, *11*, 85 – 95.
[36] a) H. Motoshima, B. J. Goldstein, M. Igata, E. Araki, *J. physiol.* **2006**, *574*, 63 – 71; b) S. M. Hadad, L. Baker, P. R. Quinlan, K. E. Robertson, S. E. Bray, G. Thomson, D. Kellock, L. B. Jordan, C. A. Purdie, D. G. Hardie, *BMC cancer* **2009**, *9*, 307.
[37] a) B. B. Zhang, G. Zhou, C. Li, *Cell Metab.* **2009**, *9*, 407 – 416; b) J. M. Evans, L. A. Donnelly, A. M. Emslie-Smith, D. R. Alessi, A. D. Morris, *Br. Med. J.* **2005**, *330*, 1304 – 1305.
[38] T. Chen, Y. Wong, *Cell. Mol. Life Sci.* **2008**, *65*, 2763 – 2775.
[39] H. Wu, X. Li, W. Liu, T. Chen, Y. Li, W. Zheng, C. W.-Y. Man, M.-K. Wong, K.-H. Wong, *J. Mater. Chem.* **2012**, *22*, 9602 – 9610.
[40] T. Chen, Y. S. Wong, *Biomed. Pharmacother.* **2009**, *63*, 105 – 113.
[41] C. Qian, J.-Q. Wang, C.-L. Song, L.-L. Wang, L.-N. Ji, H. Chao, *Metallomics* **2013**, *5*, 844 – 854.
[42] W. Liu, X. Li, Y.-S. Wong, W. Zheng, Y. Zhang, W. Cao, T. Chen, *ACS Nano* **2012**, *6*, 6578 – 6591.
[43] L. He, Y. Huang, H. Zhu, G. Pang, W. Zheng, Y.-S. Wong, T. Chen, *Adv. Funct. Mater.* **2014**, *24*, 2754 – 2763.

Received: December 12, 2014
Published online on ■■ ■■, 0000

FULL PAPER

Medicinal Chemistry

*Yuedan Liu, Yi Luo, Xiaoling Li,**
*Wenjie Zheng, Tianfeng Chen**

■■ – ■■

Rational Design of Selenadiazole Derivatives to Antagonize Hyperglycemia-Induced Drug Resistance in Cancer Cells

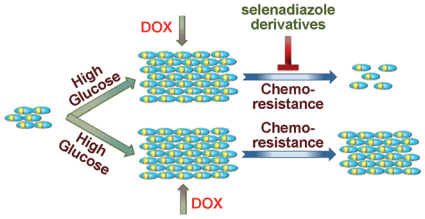

Se shall overcome: An effective strategy to design selenadiazole derivatives with the potency to overcome hyperglycemia-induced drug resistance in cancer cells via regulation of ROS-mediated signaling pathways is reported.